



INTRALAB MEMORANDUM

TO: CSDL Space Station Distribution

MEMO NO: Space Station 87-20

FROM: J. Paradiso

DATE: November 20th, 1987

SUBJECT: Methods of Smoothing CMG Gimbal Rates Calculated by Linear Programming

ABSTRACT

Recent studies in momentum management conducted on the VAX Space Station Simulator have renewed interest in the features and performance of the CSDL-developed hybrid CMG/RCS steering/selection procedure. Since the linear program employed by the steering/selection law can often substantially change its solution while the CMGs are in motion, appreciable high-frequency noise can appear in gimbal rate profiles. While this artifact has little effect on momentum management results (where gimbal rates are integrated), it can introduce potential problems when commanding real CMGs onboard a flexible spacecraft. This report examines a means of changing variables in the linear program to create a steering law that improves the continuity of calculated CMG gimbal rates.

Methods of Smoothing CMG Gimbal Rates Calculated By Linear Programming

1) Introduction

Previous work [1],[2],[3],[4] has demonstrated several advantages of resolving the CMG steering problem through linear programming; ie. implicit consideration of upper bounds on decision variables, intrinsic optimization of a linear objective function, highly flexible system definition and reconfiguration abilities, and the possibility of automatically commanding additional actuator families (ie. jets) when needed. Refs. [1 → 4] detail many applications of the above-listed features that significantly enhance the attitude control capabilities of CMG-bearing vehicles such as the Space Station.

The optimal solution to a linear programming problem will specify non-zero decision values for a subset of available activity vectors. A basis of three activity vectors (assuming 3-axis rotational control) is always selected with intermediate decision values, together with other activity vectors (where necessary) saturated at their upper bounds. When using linear programming to specify CMG motion in response to an input torque request, the activity vectors represent torque authorities of individual CMG gimbals, and their decision variables are the corresponding gimbal rates (although Refs. [1] and [2] solved for CMG gimbal displacements in response to input vehicle rate-change commands, the situation was analogous).

For small torque commands, the linear program will generally pick only a basis of three CMG gimbals to be run at modest rates; these three gimbals represent the optimal solution with respect to the current linear objective coefficients. After the assigned CMG gimbals have moved by a small amount, the linear selection is repeated. Now, however, the objective coefficients and activity vectors can be considerably different, due to the nonlinear nature of the global problem (note that the linear program solves only a local tangent approximation at each time step). As a result, the three CMG gimbals chosen to solve the updated problem may be entirely different from those in the original solution. This behavior can also appear at higher torque levels, where additional activity vectors included at their upper bounds can

similarly modulate on-and-off as the nonlinear character of the problem dynamically influences the tangent approximation.

When it occurs, this rapid switching of the selected gimbals can create an excessively noisy gimbal rate profile, with CMG gimbals repeatedly turned on and off after only a small number of simulation time steps have elapsed. Although the gimbal angles themselves generally follow adequately smooth trajectories, driving actual CMGs with such a spiky rate command may excite structural resonances, reduce hardware lifetime, and lead to a considerably elevated power dissipation. Pseudoinverse-based CMG steering laws also use tangent approximations to the nonlinear global problem, but they continually assign rates to all CMG gimbals (due to the intrinsic 2-norm optimization), thus frequently yield a smoother response than the linear program (which prefers to consider a subset of only 3 gimbals in its solution).

A geometric interpretation of linear programming [5] provides additional insight into this problem. The set of linear constraints which define the torque command and actuator bounds (ie. see Eq. 1 in the next section) may be described by a convex hyper-polyhedron in gimbal-rate space (which is dimensioned to the number of available gimbals). Each face of the polyhedron is determined by a linear combination of activity vectors (ie. gimbal output torques) that satisfy these constraints. Since the objective function specifies a unique direction to minimize in gimbal space (or maximize; let's assume the former here), the point on the polyhedron having minimum projection along the objective direction represents the optimal solution to the constraints. Since the polyhedron is convex, this optimal point will always be a vertex (unless a face is orthogonal to the objective direction, causing each point on that face to be equally optimal; in this case, the particular linear program incarnated here will still pick a vertex). This vertex condition also describes the reason why linear programming prefers to pick only 3 gimbals to answer the 3-axis torque constraint (in the absence of upper bounds, all vertices will correspond to solutions with 3 non-zero gimbal rates).

As the CMG gimbals rotate, the shape of the polyhedron changes (but it remains convex, at least in the linear tangent space), and the objective direction shifts, causing different vertices to project optimally. When another vertex becomes optimal, the chosen solution can change dramatically, resulting in a corresponding discontinuity in gimbal rates.

The pseudoinverse, on the other hand, is subject to the same equality constraint (without bounded variables), but minimizes an entirely different objective (the sum

of gimbal rates squared). This can essentially be interpreted as a minimum-radius condition, and when applied to the constraint polyhedron, it no longer suggests selection of a vertex as being optimal; in fact, it will probably most often choose a point on the midst of a face. This results in a solution involving all gimbals (not just a subset of 3), and produces a more continuous variance as the constraints vary; the minimum-radius point will track smoothly as the face changes orientation, and jump to another face only after a significant change in the constraint (ie. a different torque command is specified). In comparison, the vertex-jumping behavior implicit in linear programming can frequently produce substantially different solutions as the gimbals move.

One straightforward method of smoothing the gimbal rates output from the linear program is to low-pass filter the gimbal rate commands before applying them to the CMGs. Because the gimbal angle history appears quite reasonable on average, a modest filtering of the gimbal rates should create a sufficiently smooth set of CMG directives (most gimbal "noise" is at high frequency). In order to retain full control bandwidth, however, the steering law may be required to assign gimbal rates more frequently (potentially reducing the update period and increasing the computational burden). During on-orbit space station operation, the required torques are generally fairly small and steady (considerable reduction of control bandwidth might actually be necessary to avoid interaction with low-frequency structural modes), thus such a gimbal rate smoothing filter might be an appropriate approach.

Another method, however, presents a possibility of achieving smoother gimbal rate profiles without requiring an output filter. This technique involves a change-of-variables in the linear program; instead of solving for the CMG gimbal rates required to achieve an *absolute* torque request, we now use the linear program to pick the *change* in CMG gimbal rates needed to realize a desired *change* in vehicle torque. Because the linear program is intrinsically attracted to the solution that produces decision values of zero (ie. no CMG motion in the absolute torque formulation with positive objective coefficients), it will now prefer to invoke minimal change in the CMG gimbal rates, thereby yielding a smoother gimbal rate response. The following sections of this report present the details required to implement this strategy, and examine its performance in a series of simulation examples.

2) Procedure

This section outlines the modifications that must be performed to the CMG steering logic in order to enable the linear program to operate properly under the

change of variable. Details of the original linear programming logic and steering law may be found in [2]; the following text assumes that the reader is already familiar with these principles.

The equality constraint that is used in the baseline steering law to solve torque requests (actually, we solve for acceleration in practice, but the torque convention will be retained here for simplicity) may be stated similarly to Eq. 25 of [2]:

$$(1) \quad \sum_{j=1}^N A_j x_j = \underline{M}$$

$$|x_j| \leq x_{\max_j}$$

Where...

N = # CMG gimbals considered

A_j = Output torque of CMG gimbal #j at unit gimbal rate

x_j = Gimbal rate for CMG gimbal #j

x_{\max_j} = Peak gimbal rate for CMG gimbal #j

\underline{M} = Vehicle Torque Request

Changing variables in this relation to steer CMGs under a delta torque scenario is straightforward:

$$(2) \quad \sum_{j=1}^N A_j \Delta x_j = \underline{\Delta M}$$

$$-x_{\max_j} - x_j \leq \Delta x_j \leq x_{\max_j} - x_j$$

Where...

Δx_j = Change in gimbal rate for CMG gimbal #j

$\underline{\Delta M}$ = Change in vehicle torque request

N, A_j, x_j, x_{\max_j} are as defined in Eq. 1

The objective function used in the baseline steering law (as described in Ch. 3 of [2]) contains components that act to minimize inner gimbal angles, avoid gimbal

stops, and prevent singular states. If one applied this objective directly to Eq. 2, the initial selection would indeed pick gimbal rates satisfying these criteria. A problem, however, arises after the gimbals are in motion. Although it becomes increasingly more costly to select additional gimbal action Δx_j in a direction that approaches a problematic configuration (ie. singularity or stop vicinity), the linear program is not forced to specify gimbal motion in the opposing direction (ie. avoiding the stop or singularity). Since the linear program tends toward a minimum-action solution, the small ΔM commanded to compensate nonlinear effects after the gimbals start rotating generally precipitates correspondingly small Δx_j . This creates a situation where the initially selected gimbal motion is not substantially altered; the small trimming needed to compensate the CMG nonlinearity (assuming the commanded torque M doesn't change significantly) doesn't appreciably affect the trajectory of the chosen CMGs. In a certain sense, this is a direct manifestation of the original purpose in changing decision variables; the steering algorithm has developed an "inertial" tendency to keep gimbal rates constant, admitting only minor alterations where necessary. This often creates additional problems, however; ie. if a gimbal is initially selected to move in an "innocent" direction, things can later become ominous if its trajectory is not altered before it eventually approaches a stop or participates in creating a singular configuration.

This situation has been addressed by allowing the cost opposing the worst-positioned CMG gimbal to become negative. As illustrated in [2], every CMG gimbal has two associated objective factors corresponding to opposite senses of gimbal rotation. Each of these costs reflects the optimality of moving a CMG gimbal in the corresponding direction. If one cost is high, indicating an impending problem, the other cost should be lower, provided that motion in the opposite sense will not invoke another difficult configuration. The "urgency" of moving a gimbal is thus reflected in the difference between its pair of associated costs; if this difference is excessively large, it is determined that the responsible CMG gimbal is approaching trouble that can be averted by reversing its direction of rotation. This is indeed what is performed to prevent the above-mentioned tendency toward a static solution. When the cost difference of a gimbal pair increases beyond a preset threshold, the lower cost of the pair is allowed to go slightly negative, thereby encouraging its selection and subsequent gimbal reversal. In order to avoid chaotic solutions which slam negative-cost gimbals at peak rates in order to glean the maximum benefit from the inverse-sign objective factor, the upper bound regulating the gimbal rate-change in that direction is reduced, clamping corresponding gimbal activity to a reasonable level. In addition, only one cost factor out of the entire CMG ensemble is allowed to go negative per selection; the low-cost factor associated with the maximum cost difference is chosen.

The above procedure is summarized below using the conventions of [2]:

Define:

$$\delta c_j = |c_j^+ - c_j^-|$$

$$c_j^{smin} = \text{minimum}\{c_j^+, c_j^-\}$$

$$(3) \quad c_{neg_j} = c_j^{smin} - \lambda \delta c_j$$

$$c_{neg_{jmin}} = \text{minimum}_{(j)}\{c_{neg_j}\}$$

$$\text{IF } c_{neg_{jmin}} < -C_0 \text{ THEN } \left\{ \begin{array}{l} c_{jmin}^{smin} \rightarrow c_{neg_{jmin}} \\ UB_{jmin}^{smin} \rightarrow \frac{UB_{jmin}^{smin}}{\kappa} \end{array} \right.$$

Adjustable Factors...

λ = Negative cost skew factor

C_0 = Negative cost threshold

κ = Upper bound attenuation factor for negative costs

The upper-bound attenuation factor κ should be made to decrease toward unity as the magnitude of the torque request increases, allowing the system to marshal full response to large input commands.

The logic of Eq. 3 provides the delta torque steering method a dynamic means of modifying its strategy in accordance with the objective function. Because of its inherent "inertial" characteristic, the delta torque method will tend to minimize perturbation of the CMG gimbal rates until the threshold ($-C_0$) in Eq. 3 is exceeded and a cost is made negative.

Although the zero gimbal rate solution served as an intrinsic attractor for absolute torque steering, the delta torque method has no special preference for zero rates. This results in an effective loss of damping, allowing the CMG system to be "pumped" to higher gimbal rates and eventual chaotic behavior after each major change in the solution (caused by a shifting torque request or negative cost factor). It is clear that any practical steering law formulated in the delta torque domain must contain some means of dissipating energy in order to keep gimbal rates from being excessively boosted.

The objective function was modified to accommodate such gimbal damping by adding a term to the objective definition that opposes each gimbal rate. The cost factor definition (Eq. 30b of [2]) then becomes:

$$(4) \quad c_{j,s} = K_0 + K_A F_{Angle}(j,s) + K_S G_{Stops}(j,s) + K_L Y_{Lineup}(j,s) + K_R Z_{GRate}(j,s)$$

Where...

$$Z_{GRate}(j,s) = \begin{cases} |x_j| & \text{If } (s)(x_j) > 0 \\ 0 & \text{Otherwise} \end{cases}$$

x_j = Current gimbal rate for gimbal #j

s = Sense of gimbal rotation considered (± 1)

The Z_{GRate} term added in Eq. 4 increases with the assigned gimbal rate for additional rotation in the current direction of gimbal motion, effectively penalizing solutions which would specify higher gimbal rates, and encouraging prompt gimbal deceleration (re. negative cost from Eq. 3) after significant gimbal displacement.

Other innovations were incorporated to damp excessive gimbal chattering as momentum saturation was approached; these included both boosting K_0 (Eq. 4) and reducing the allowed magnitude of negative costs as the system saturates. Since both of these effects were made proportional to the increase in saturation beyond 80% momentum capacity, they are of little relevance to the test presented in the following section (which didn't drive the system beyond these extremes).

In examining the detailed performance of the linear programming process with negative cost factors, a correction was made to the invite loop of the simplex procedure detailed in the flow chart presented in Fig. 5 of [2]. The relation **SGN = sign(F)**, which determines the best rotation sense to use when inviting candidate gimbals into the solution, should read:

$$(5) \quad SGN = \text{sign}\{2F - C_I^+ + C_I^-\}$$

Where...

I = Index of invited activity vector

C_I^\pm = Cost of invited activity in the \pm direction

This function will yield a value of +1 if a positive rotation determines a greater cost gradient (CG) than a negative rotation, and -1 if vice-versa. The previous formulation is accurate when all cost factors are positive (ie. SGN is always selected such that F projects positively, yielding the only chance for a positive cost gradient in this case), but may cause convergence to suboptimal solutions when negative costs are allowed. Eq. 5 directly accounts for the different cost factors in each direction, thus any effective gain from negative costs are considered.

2) Simulations

In order to examine the effect these concepts might produce in practical application, several simulations were performed assuming the Dual Keel Space Station to be controlled by an array of 6 parallel-mounted double gimballed CMGs initially in a zero-momentum state with outer gimbal axes aligned along vehicle pitch. Parameters defining the Dual Keel configuration and associated CMGs are identical to those applied in [3]. The linear program was not allowed to select jets in these tests (no examples ran the CMGs into saturation), but the logic to answer vehicle rate-change commands through hybrid solutions was left intact for this contingency.

a) Attitude Slews About Pitch/Roll

The first set of simulations run the system at fairly high torque by performing a fast attitude slew about the vehicle pitch and roll axes. Vehicle rates of 0.0055 deg/sec are linearly built about pitch and roll within approximately 35 seconds, then removed within a similar time frame, establishing a constant vehicle acceleration of $\pm 0.00016^\circ/\text{sec}^2$ (this results in a net torque of about 500 ft-lb due to the large Dual Keel inertias). Vehicle environment and control (if necessary) were updated at 80 msec. intervals:

Fig. 1 shows the gimbal results for this maneuver as managed by commanding absolute torque in a similar fashion to the relevant examples of [3]. The inner gimbal angles are seen to advance in a "braided" fashion, where an initial solution primarily advances one gimbal until it becomes slightly more expensive than its colleagues, thereby causing it to be halted and substituted by another, and so on.... This process stepwise increases the inner gimbal angles (which are the only means of attaining pitch torque) until the input command reverses direction after they near 40° . Their reverse trajectory is not so uniform (since the extreme expense of increasing inner gimbal angles no longer limits the solution), yet most inner gimbals again approach zero deflection at the close of the test. Outer gimbals are seen to smoothly congregate together at the midpoint of the simulation (indicating impending saturation), and thereafter return to the neighborhood of their initial positions.

Although the gimbal angle profiles appear reasonably well-behaved, the gimbal rates look significantly more chaotic, forming a series of narrow spikes extending up to the 5.2 deg/sec maximum (note the switch in sign of inner gimbal rates after the input command was reversed). These spikes were caused by changes in the linear programming solution encountered at each control iteration, as predicted in the introduction of this report (the inner gimbal "stepwise" advance mentioned above is a physical consequence of this behavior). Driving a system of actual CMGs with these commands could certainly be problematic. Note, however, that the smoothness of the gimbal angle profiles indicates that a modest filtering of the calculated gimbal rates might yield a similarly smooth response. Other examples of noisy gimbal rate commands produced from absolute torque inputs were presented and analyzed in [4].

Fig. 2 presents a set of gimbal plots for the same maneuver performed under delta torque steering. An entirely different behavior is seen to emerge. Looking first at the inner gimbal angles, one notices that the initial commands were fulfilled primarily by advancing CMG #5. After it reached a deflection of about 40° , however, it became sufficiently expensive to trigger the negative cost logic of Eq. 3, encouraging it to be selected in the opposite direction, while advancing two other CMGs from zero deflection to maintain the commanded torque. This behavior continued across the entire run, causing a steady-state inner gimbal scissoring as successive CMGs ramped up until their costs in the reverse direction went negative. The outer gimbal angles also hint at some scissoring action, however any effect is much more subdued (outer gimbal deflections are not penalized; the major terms in their objective are due to lineup & singularity avoidance).

Fig. 1) Attitude Slew with Absolute Torque Steering

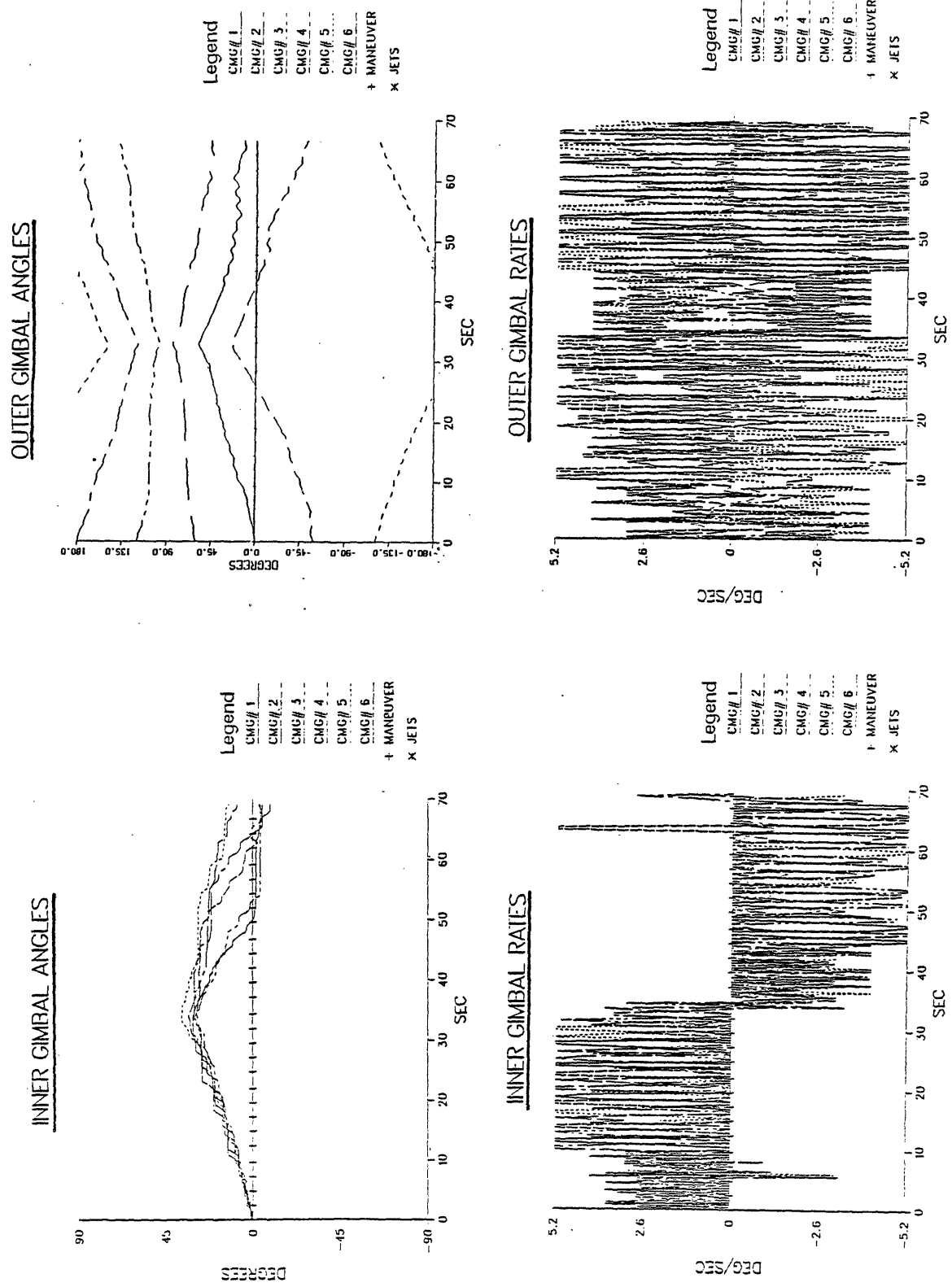
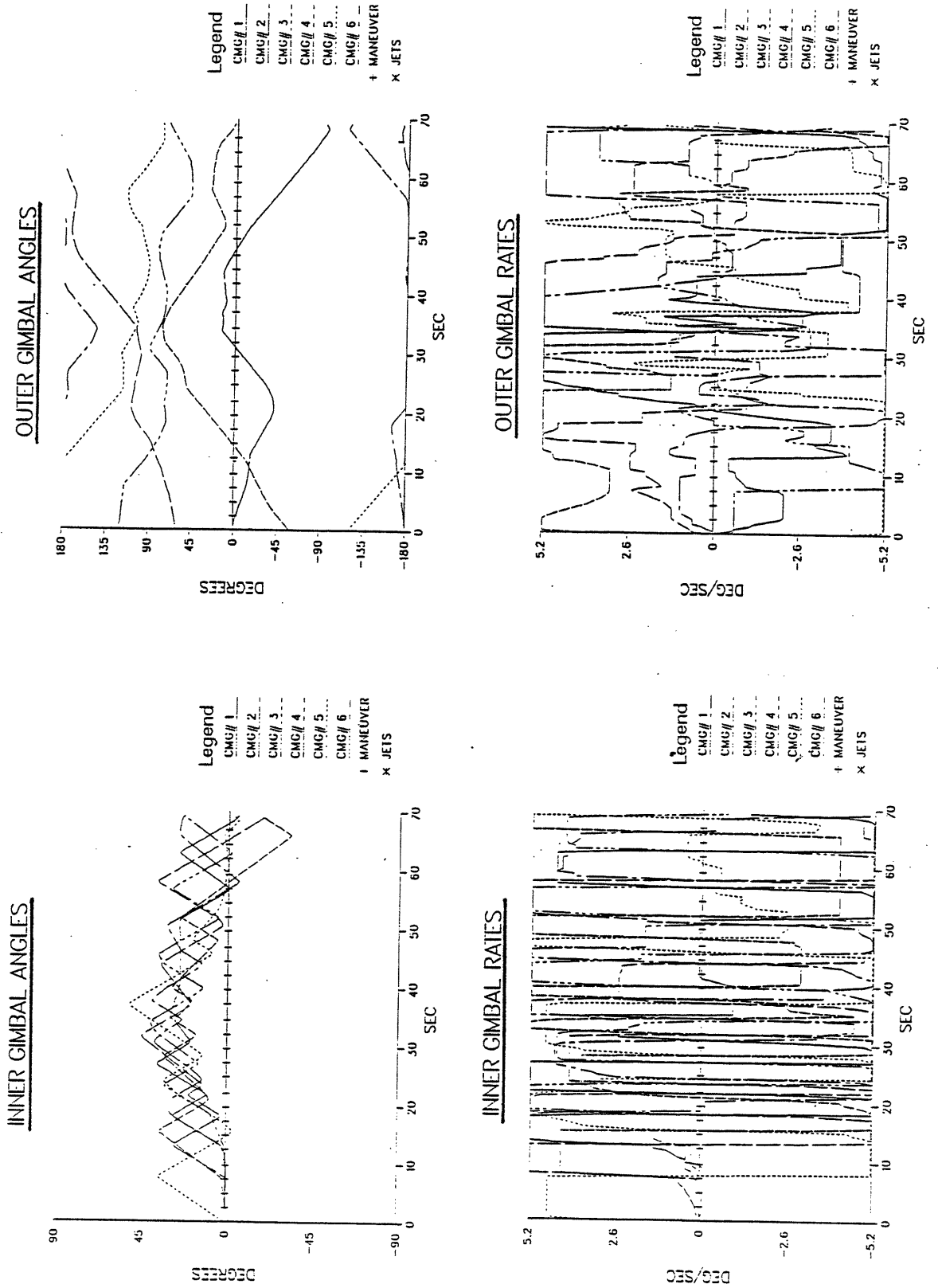


Fig. 2) Attitude Slew with Delta Torque Steering



The companion gimbal rates show much less high frequency component when compared to the absolute torque results; the "spikes" are essentially gone. These rates, however, do frequently move between their positive and negative limits as gimbals are scissored back and forth at maximum clip, indicating excessive energy being pumped into the system, thus emphasizing the need for damping.

The next test tries to tame this scissoring by increasing K_R in Eq. 4 (it was almost negligible in the previous test), thereby adding significant rate-damping encouragement to the objective. In addition, the bound attenuation factor κ in Eq. 4 was boosted to 3 (it was set to unity in the above example, allowing scissoring at maximum rates), significantly limiting the adjustment of gimbal rates associated with negative costs.

The results, as given in Fig. 3, are quite dramatic. Both inner and outer gimbal angle profiles become quite smooth and well-behaved. The calculated rates are the most continuous yet seen; indeed, they often vary smoothly across the maneuver and exhibit comparatively little significant discontinuity. Although gimbal rates are non-zero at the close of the run (they are essentially performing null motion), little evidence of excessive energy pumping is evident in this example, indicating successful compensation attained from the rate-damping objective and upper-bound attenuation.

Fig. 4 shows the vehicle rates resulting from the previous three examples. In spite of the differing gimbal trajectories pursued in each example, all rate histories appear nearly identical, and the peak pitch/roll rates of 0.0055 deg/sec were linearly achieved and removed with little disturbance.

b) Orbital Simulations

In order to examine the performance of delta torque steering in a more practical context, longer simulations were performed over an orbital period, throughout which the Dual Keel model was commanded to hold constant LVLH attitude in the presence of aerodynamic and gravity gradient torques. Orbital altitude was assumed to be 400 km, and the target attitude in the initial tests was chosen to produce torque equilibrium about the pitch axis. Vehicle fabrication axes were used in the other coordinates; this introduced significant Euler coupling across the orbit, which required the CMGs to cyclically absorb 70% of their momentum capacity. More details on the orbital environment and attitude controller used in these examples can be found in Sec. (c) of [3].

Fig. 3) Attitude Slew with Delta Torque Steering
Limit excursions with negative costs

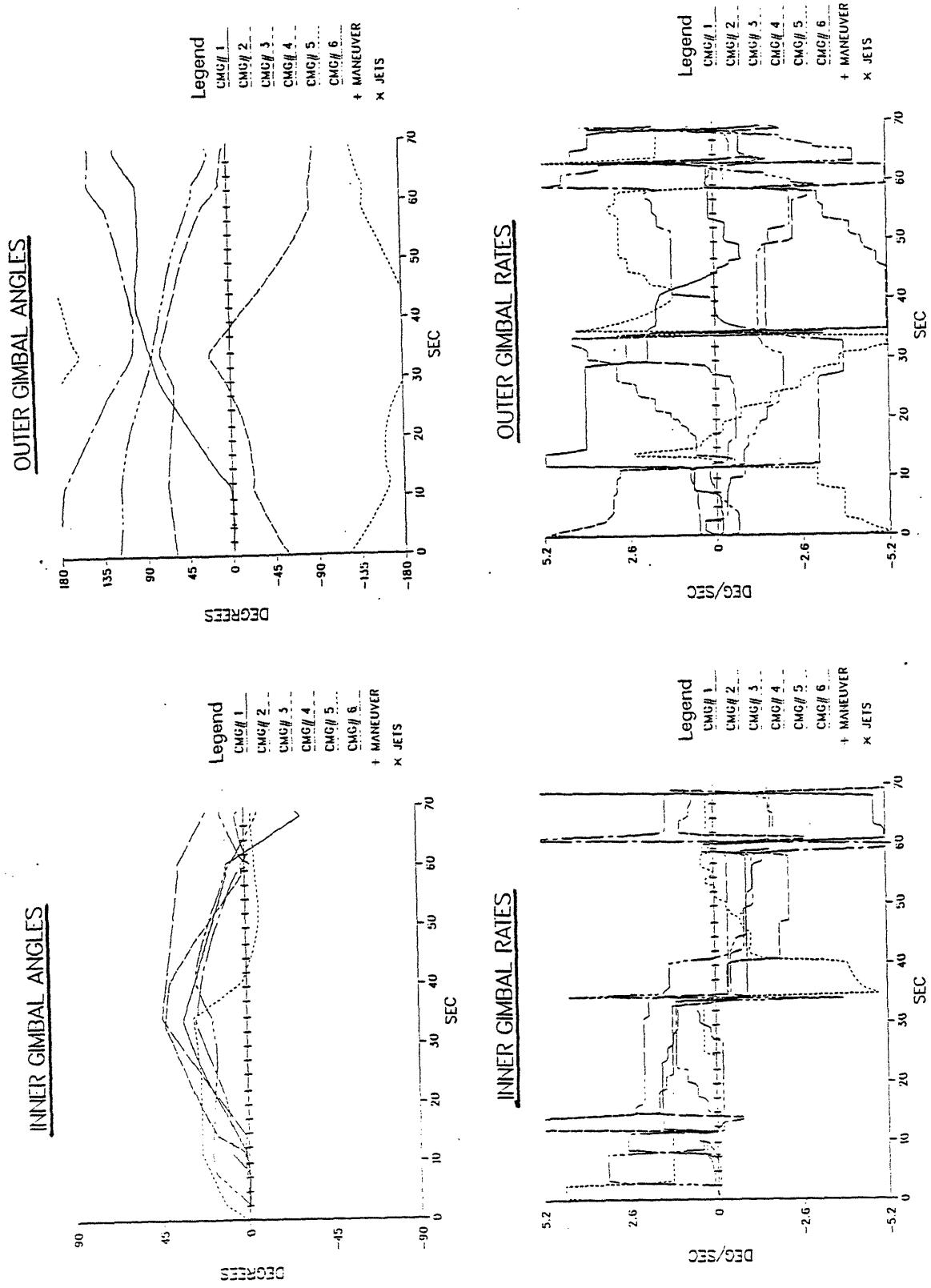
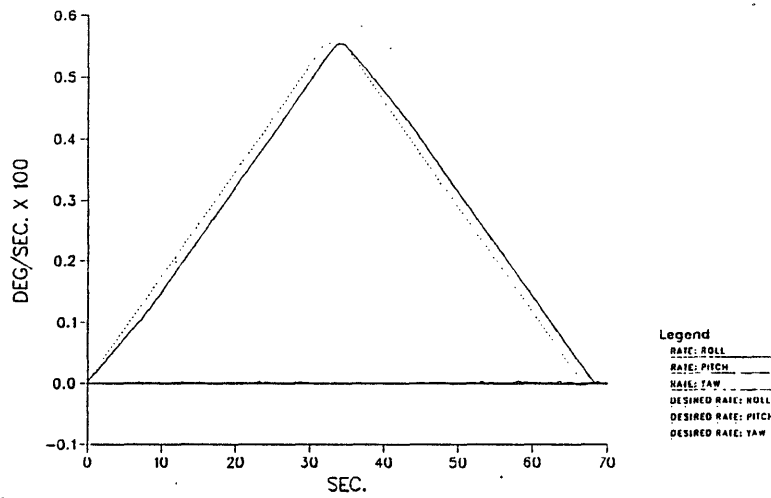
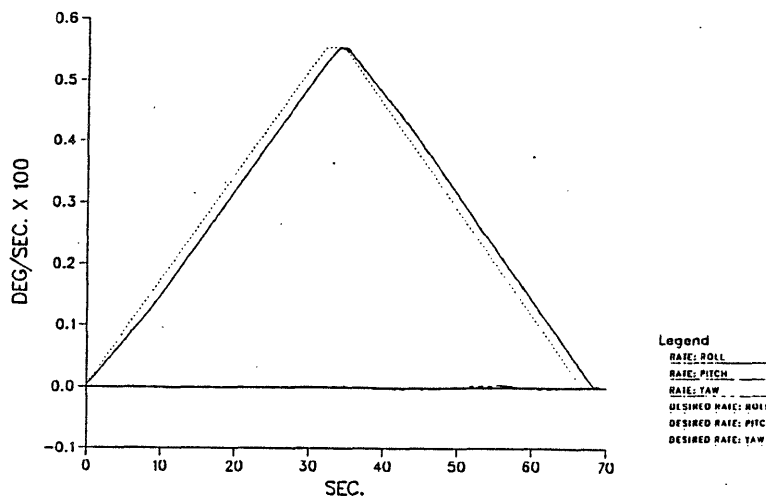


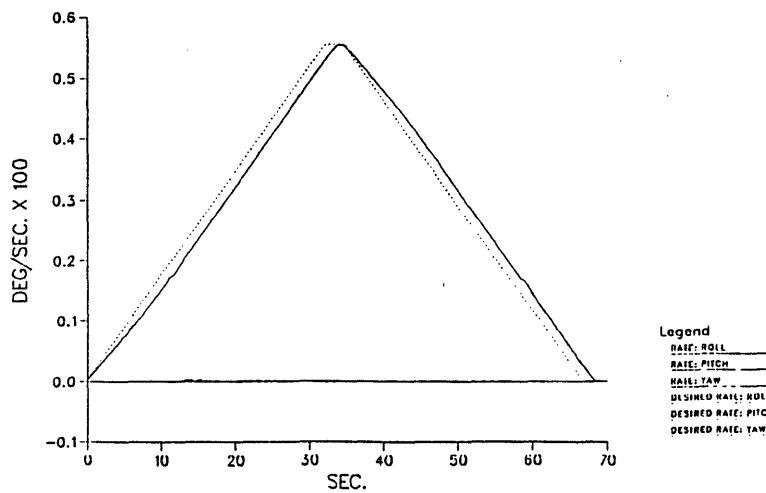
Fig. 4) Vehicle Rates Resulting from Attitude Slew Tests



a) TRIANGLE MANEUVER; STEER ABSOLUTE TORQUE



b) TRIANGLE MANEUVER; DELTA TORQUE STEERING



c) TRIANGLE; DELTA TORQUE W. BOUNDS

Fig. 5 shows gimbal parameters resulting from such an orbital attitude hold under absolute torque steering. Assumptions made in this simulation were nearly identical to those of Fig. 22 in [3], thus we see analogous gimbal behavior. Because the pitch torques are in equilibrium, no significant inner gimbal activity is evident. Outer gimbals are seen to rotate through large angles, however, in order to null the Euler torques about roll and yaw. Although the gimbal trajectories appear reasonably smooth, the outer gimbal rates do exhibit some characteristic chatter, although at a smaller level than seen in the previous test (these examples are run over a much longer duration, thus involve considerably less torque). Note the factor 10 reduction of scale on all gimbal rate plots presented with on-orbit tests; y-axes now range ± 0.5 deg/sec. Vehicle rates (not plotted here due to lack of space) remained under 4×10^{-5} deg/sec.

The next investigation applies the delta torque approach as perfected in the example of Fig. 3. A considerably noisier result is gleaned here, however, as seen in Fig. 6. Initially, the inner gimbal of CMG #4 was steadily advanced, while others were slowly moved about to null residual torques. After CMG #4's inner gimbal reached 12° , the cost of further advance rose high enough to invoke the logic of Eq. 3; which drove the opposing cost into negation. Since it became an effective "bargain", the inverse motion of CMG #4 was brought in at its maximum, causing it to move quickly to the opposite extreme and instigate a chaotic limit cycle of frantic scissoring. Similar behavior is observed in the outer gimbal system. Note that this scissoring, frenetic as it may seem, is nonetheless null motion, and vehicle rates were maintained below 3×10^{-4} deg/sec. Remember that these plots of gimbal rates saturate at ± 0.5 deg/sec; allowed rates may still range up to ± 5.2 deg/sec.

The above results emphasize a need for additional damping under these conditions. The test of Fig. 6 was run with an upper bound attenuation factor of $\kappa = 3$, as was found adequate in Fig. 3. Here, however, the gimbals can travel much further during a time step because of the longer 1 second update interval, causing scissoring to be reversed after nearly every control application. The discussion associated with Eq. 3 hinted that the upper bound on negative-cost activity vectors should be tightened with decreasing torque requirement; since environmental torquing is indeed quite low here, κ was increased to 100 in the following example (κ could be automatically scaled in practice). In addition, the gimbal rate objective contribution K_R (Eq. 4) was again increased to provide more gimbal damping.

Results are summarized in Fig. 7, where things appear significantly improved. Inner gimbal usage remains minimal (corresponding gimbal rates are quite smooth). Considerable scissoring is noted in the outer gimbal system, however high-energy

Fig. 5) LVLH Attitude Hold at TEA; Absolute Torque Steering

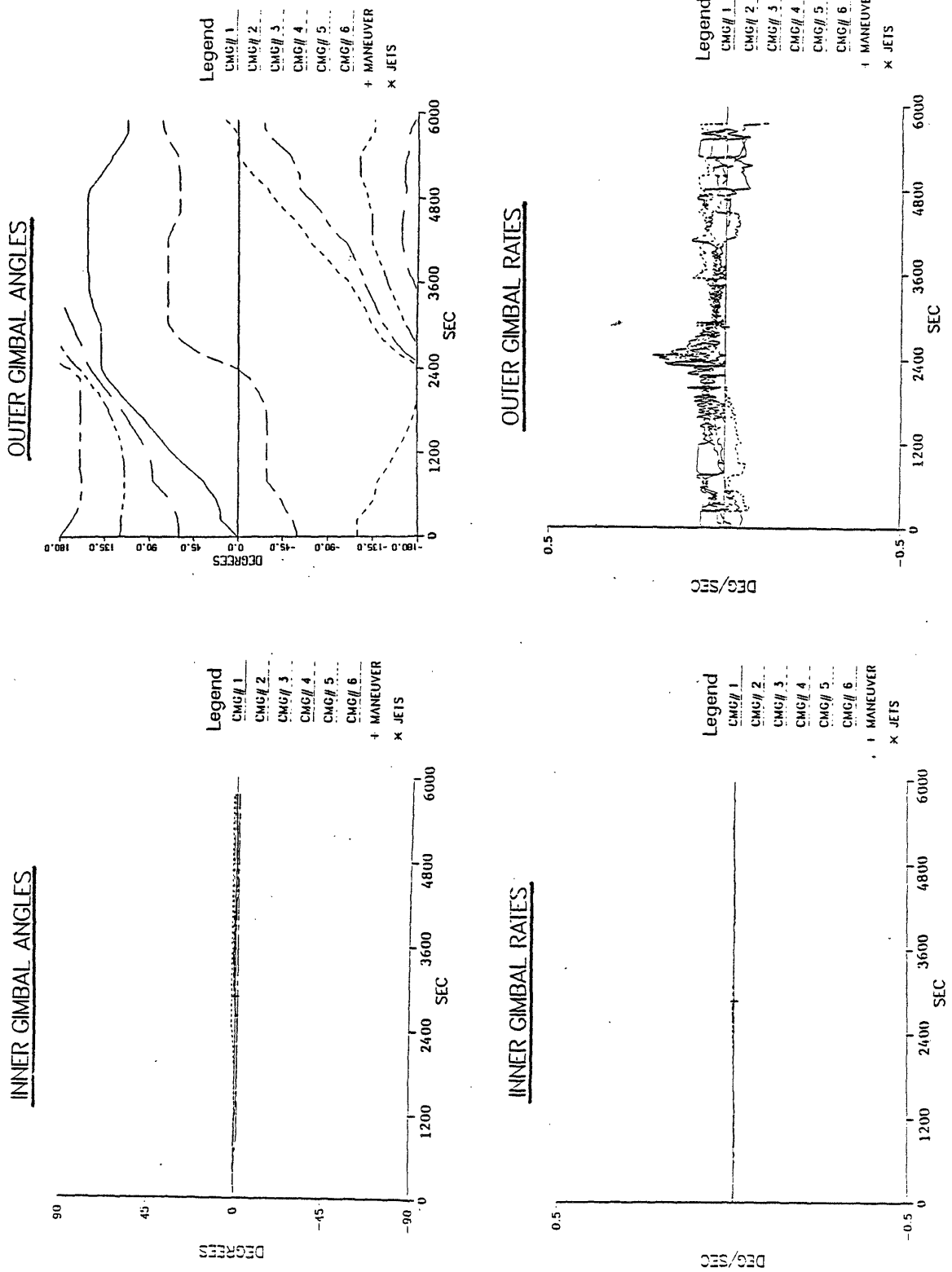


Fig. 6) LVLH Attitude Hold at TEA; Delta Torque Steering

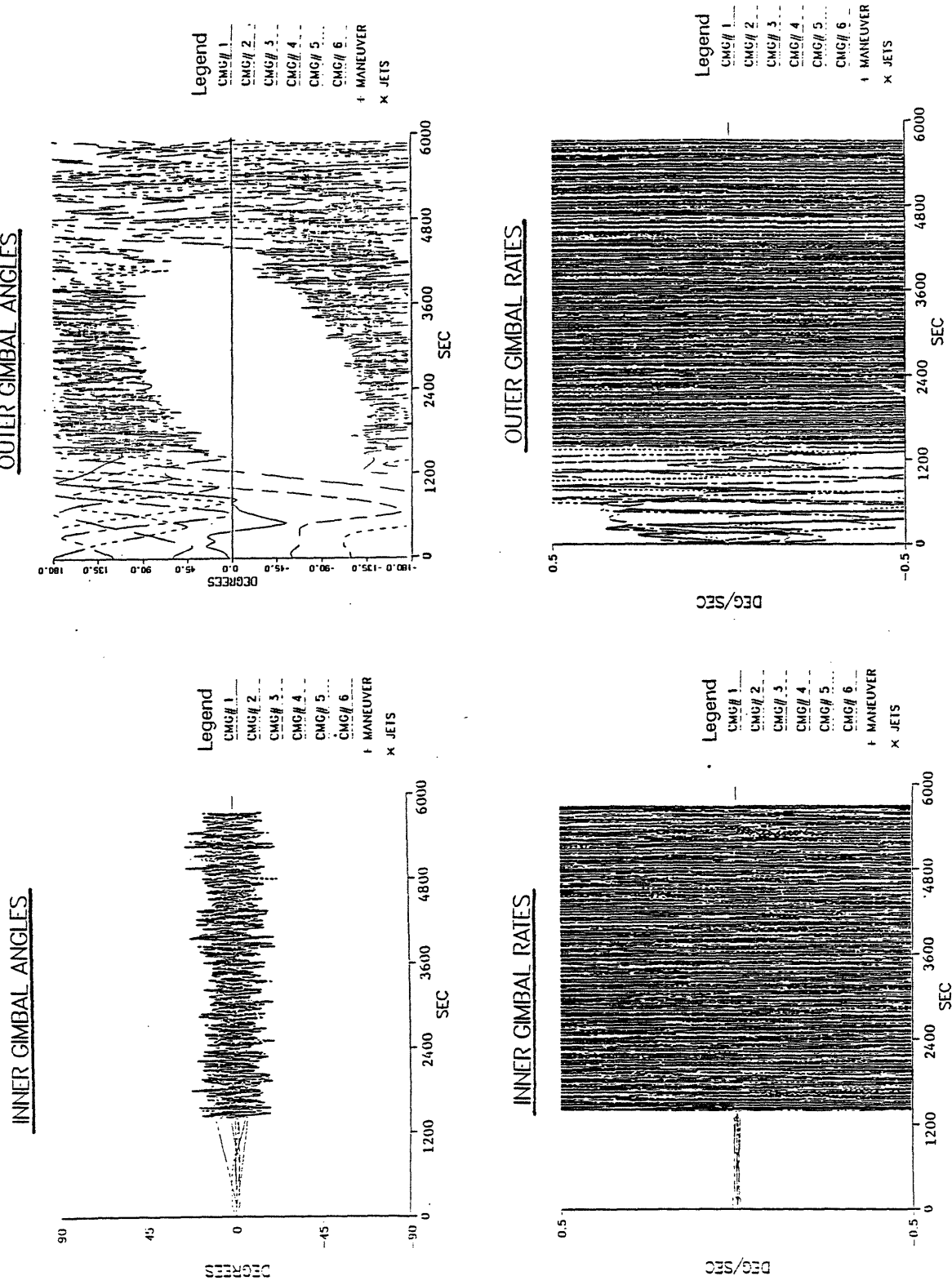
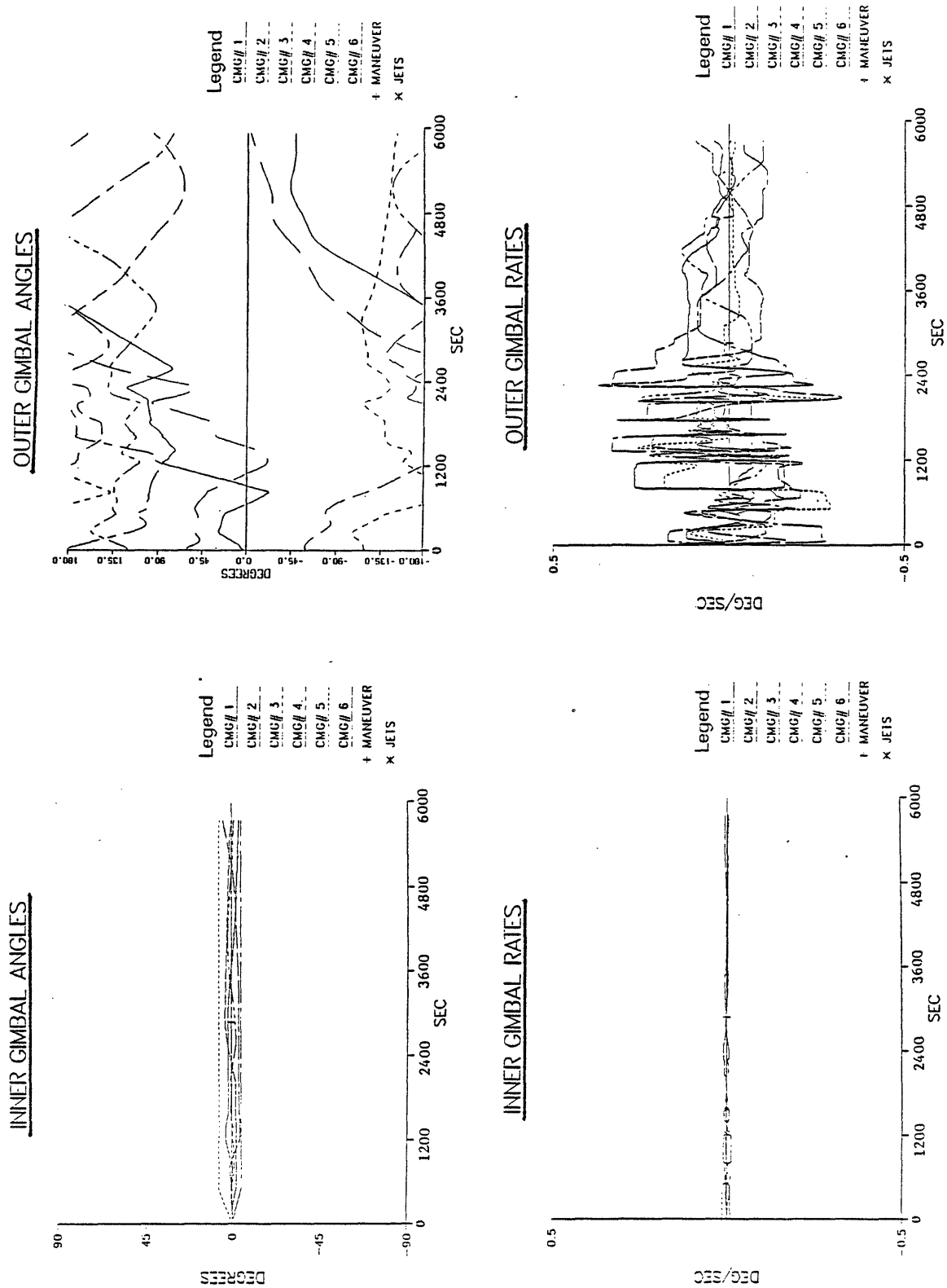


Fig. 7) LVLH Attitude Hold at TEA; Delta Torque Steering
 Increase gimbal rate penalty; Tighten limits on negative-cost gimbal



chaos is avoided, and gimbals rates appear reasonably consistent throughout most of the run (note that the update interval is a full second here, and rates stay well below a half degree per second). Gimbal rates do seem to run a little higher than encountered in the analogous absolute torque example (Fig. 5), but tend to exhibit less low-level chattering (particularly in the latter half of the test), as expected under the delta torque scenario. Vehicle rates are well stabilized and again stay under 4×10^{-5} deg/sec.

The success of the previous test encourages an attempt at a more complex simulation; the next examples offset the pitch attitude by 0.5° from torque equilibrium, requiring a steady advance of inner gimbals to offset the resulting buildup of secular pitch momentum. Fig. 8 shows the gimbal response under absolute torque steering; indeed, all inner gimbals move essentially together, and outer gimbals still rotate to null precession torques. The outer gimbal angles and rates are very similar to those seen at equilibrium (Fig. 5), including the characteristic chatter. The inner gimbal rates seem to consist of a near-zero "fuzz"; when magnified, this phenomenon begins to resemble the "spikes" seen in the rate plots of Fig. 1, indicating that the inner gimbals are indeed "stepwise" deflecting together at low torque.

The delta torque approach was applied to this situation in Fig. 9. Inner gimbals are seen to scissor as their mean deflection increases. This scissoring creates large gimbal deflections at the latter portion of the run; since all inner gimbals (which are the sole source of pitch torque with this mounting protocol) become considerably expensive to advance at large angle, the net inner gimbal reaction required to null the torque produced by reversing a gimbal trajectory likewise becomes quite expensive. The linear program does not find this solution sufficiently cost-effective until the magnitude of the negated gimbal-reversal cost grows high enough to offset the expense of the required reaction. Toward the end of the run, most inner gimbal increases become so costly that the reversal break-even doesn't happen until the worst-case gimbal nears 15° of its maximum swing (at which point its stops contribution, Eq. 32 of [2], rapidly increases, pushing the reversal cost quickly negative).

Inner gimbal rates are, however, quite smooth when compared with the corresponding "fuzz" of Fig. 8 (yet they do tend to run somewhat higher). Outer gimbal trajectories remain reasonable, although considerable scissoring is encountered early in the test. Even though gimbal rates, on average, are significantly higher than those of Fig. 8, less low-level noise is noted in this example, excepting perhaps the excessive outer gimbal scissoring encountered initially (but this seems to be primarily at lower frequency).

Fig. 8) LVLH Attitude Hold with Pitch Offset; Absolute Torque Steering

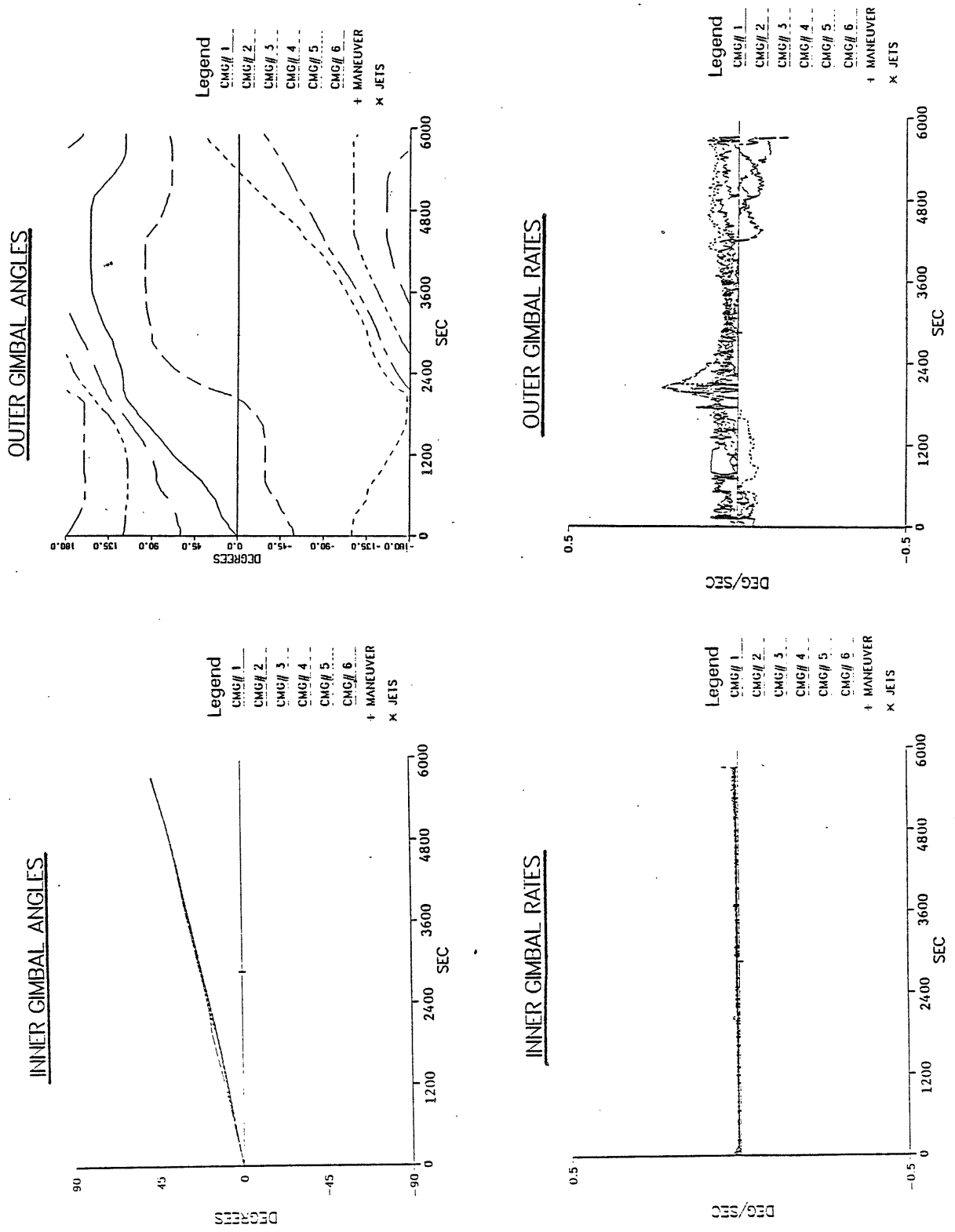
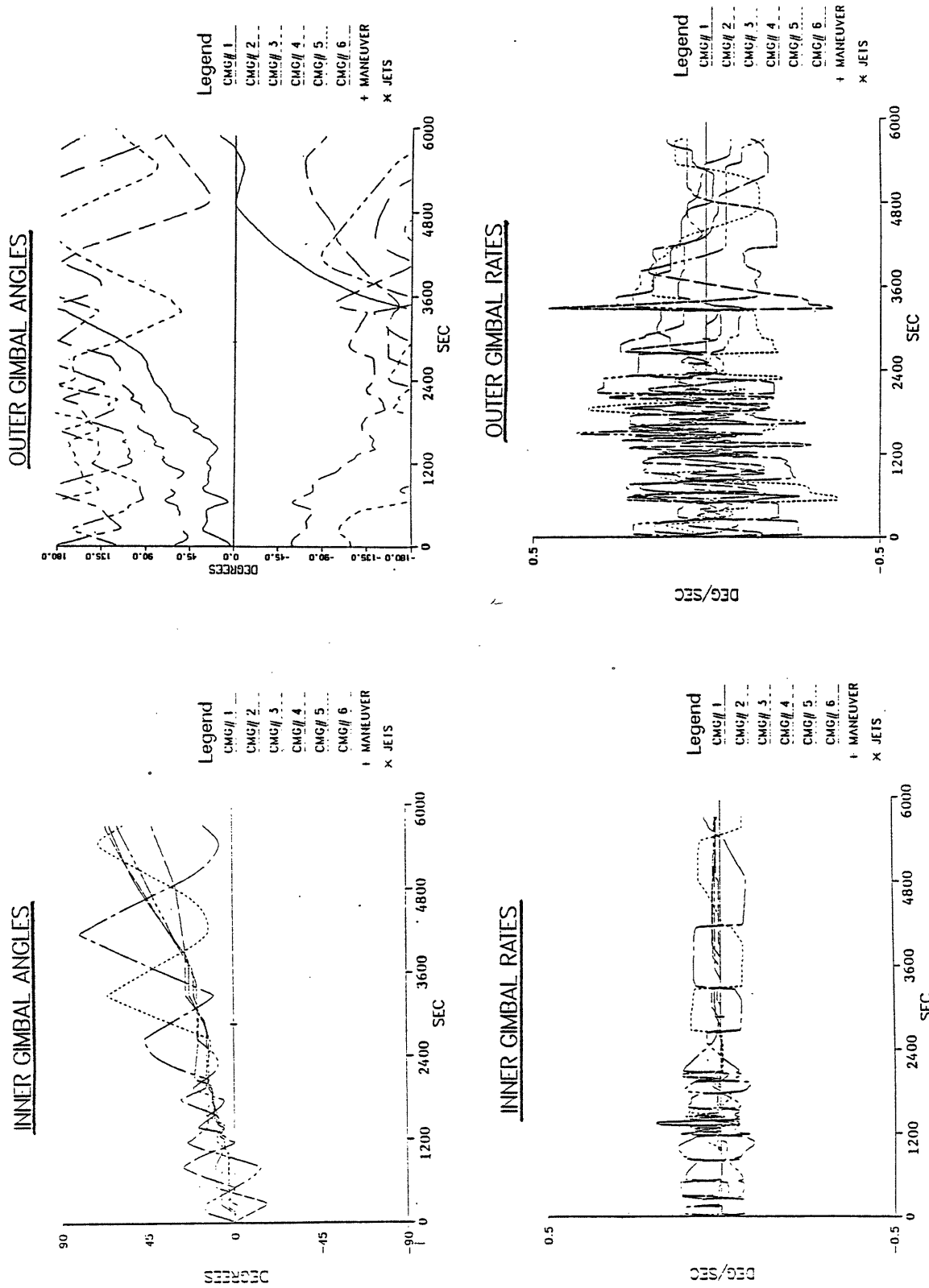


Fig. 9) LVLH Attitude Hold with Pitch Offset; Delta Torque Steering



The large inner gimbals excursions seen in this example are undesirable; in addition to nearing stop limits, large inner gimbals swings degrade the companion outer gimbals control authority. One method of reversing the inner gimbals trajectory at an earlier stage would be to unilaterally increase the overall gain on negative costs (ie. boost λ in Eq. 3). This, unfortunately, can allow the linear program to choose unphysical solutions (which were formerly too expensive), leading to eventual chaos. Boosting λ under a selective heuristic, however, could still provide some superior characteristics, while perhaps avoiding ridiculous solutions. Referring to the notation of Eq. 3:

$$(6) \quad IF \left[c_{jmin}^{-smin} > a_0 \bar{c} \right] \text{ AND } \left[\bar{c} > b_0 \right] \text{ THEN } c_{neg_{jmin}} \rightarrow g_0 c_{neg_{jmin}}$$

Where...

- \bar{c} = Average of maximum $\{c_j^+, c_j^-\}$ over all gimbals
- c_{jmin}^{-smin} = High cost paired with cost factor brought negative
- a_0 = Threshold above mean cost for boost application
- b_0 = Minimum mean cost for boost application
- g_0 = Boost factor applied to negative cost
- $[c_{neg_{jmin}}$ is the negative cost value, as in Eq. 3]

Condition (6) applies an additional gain g_0 on negative cost factors only when the aberrant gimbals has achieved a cost a_0 above the mean cost (\bar{c}) of expensive gimbals rotations. In addition, the mean cost must be greater than threshold b_0 , preventing application of this logic except in critical situations. Eq. 6 thus effectively imposes a well-defined hysteresis margin on the scissoring process at large costs.

Fig. 10 examines the application of Eq. 6 to the situation encountered in Fig. 9. In this example, a_0 was set near 2, b_0 was relatively low, and g_0 was set to 10. Inner gimbals swings are much more limited, and the scissoring frequency increases at higher inner gimbals angles as the extra gain from Eq. 6 cuts in and forces prompt trajectory reversals. Things don't get out of hand here, however, and excessive pumping (re. Fig. 6) is avoided. Outer gimbals angles and rates seem to have the same general character as the previous example (with perhaps more scissoring at the end of the run).

Fig. 10) LVLH Attitude Hold with Pitch Offset; Delta Torque Steering
Additional factor 10 gain on extreme negative costs

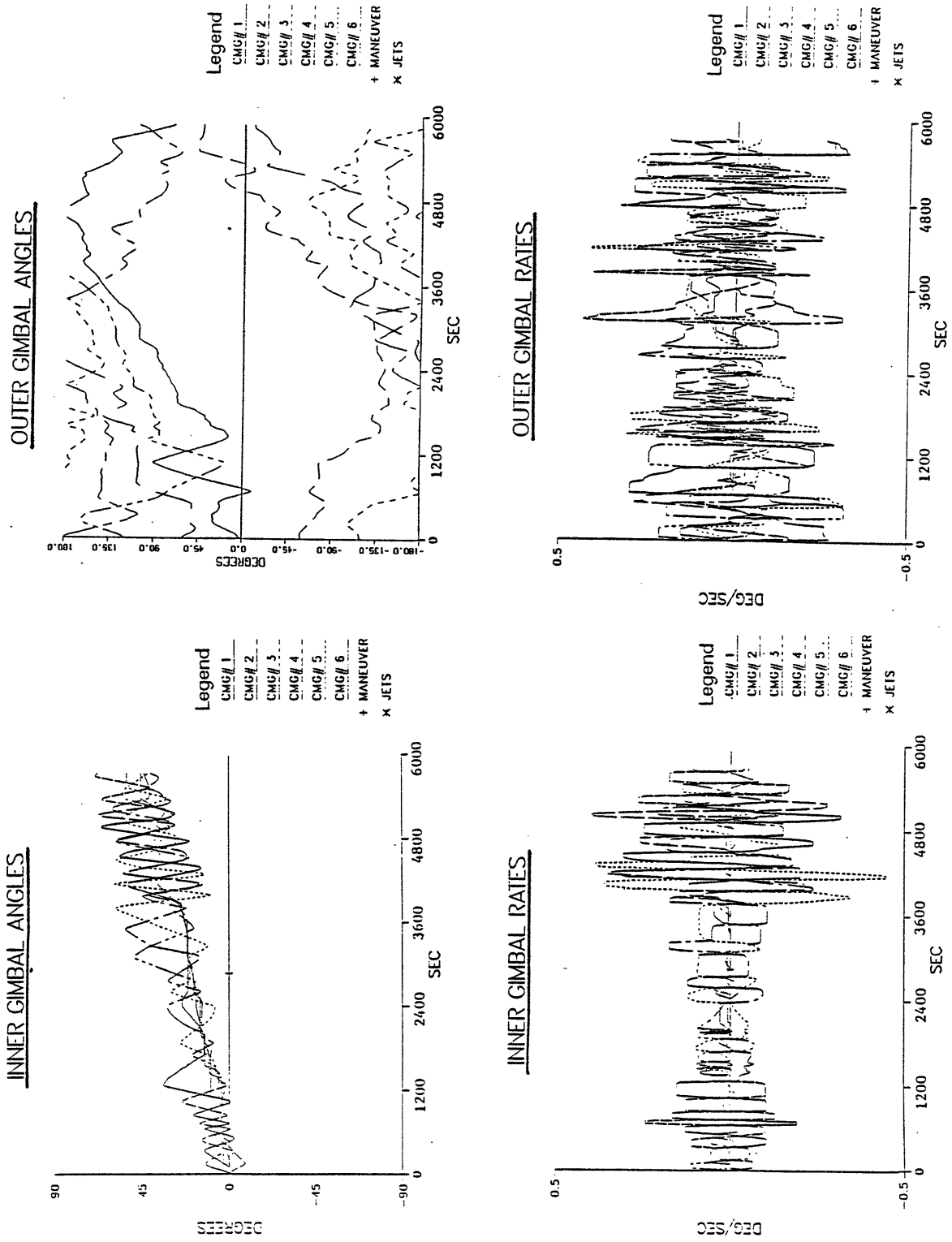


Fig. 11 is an analogous test with the gain g_0 set to 20. The tighter inner gimbal trajectory is evident; gimbals now scissor more closely to the mean deflection angle. Inner and outer gimbal rate profiles appear smaller and more consistent than encountered in Fig. 10; indeed, Fig. 11 gives the best results for this maneuver.

Fig. 12 extends this investigation by setting g_0 to 50. The initial portion of the test (up to $t = 1500$ sec) doesn't appear too different from the behavior encountered in Fig. 11. After the inner gimbal angles pass 15° , however, Eq. 6 begins to be introduced, and the large g_0 frequently reverses inner gimbal trajectories straying above the mean path. Eq. 6 now acts strongly as a sheparding function, holding all inner gimbals to an average trajectory and restoring the properties of absolute torque steering, as were shown in Fig. 8. Since the scissoring is now tightly constrained to the mean deflection, gimbal rates are much noisier, thereby defeating the original purpose for which delta torque steering was instituted. Vehicle rates throughout this test (and all other tests examining pitch displacement from equilibrium) remained under 4×10^{-5} deg/sec.

Most discussion of the previous examples centered around gimbal rates and inner gimbal deflection; little was mentioned of the singularity problem. Since the lineup avoidance amplitude (Eq. 33 of [2]) is preserved, the delta torque steering procedure should also reverse gimbal trajectories when singular states are approached (indeed, such behavior has been observed). One potential difficulty with the absolute torque steering mode concerns its minimum action policy; gimbals are moved primarily in response to input requests, and any null components tended to scale with the request magnitude. As a result, poorly positioned gimbals (as in an approach to a singular configuration) could be left untended if their motion didn't benefit the objective for solving the requested torque (ie. the gimbal response to the objective function will depend on the torque input). Conventional steering laws avoid this difficulty by always adding null motion independently of the torque request. Linear programming could potentially attain this property by allowing costs to go negative; this concept was discussed and attempted in [3] with mixed results (conclusions might improve if the correction of Eq. 5 were incorporated into simplex). The delta torque scenario, however, tends to keep CMG gimbals moving (as mentioned earlier, attracting the zero-rate solution can be difficult), thus the system is nearly always performing null motion. Since the objective function influences this gimbal activity, the system should generally steer away from singular configurations. If a problem configuration is neared, however, the continuous null motion should promptly remove the system from its vicinity (provided the singular state is escapable).

Fig. 11) LVLH Attitude Hold with Pitch Offset; Delta Torque Steering
 Additional factor 20 gain on extreme negative costs

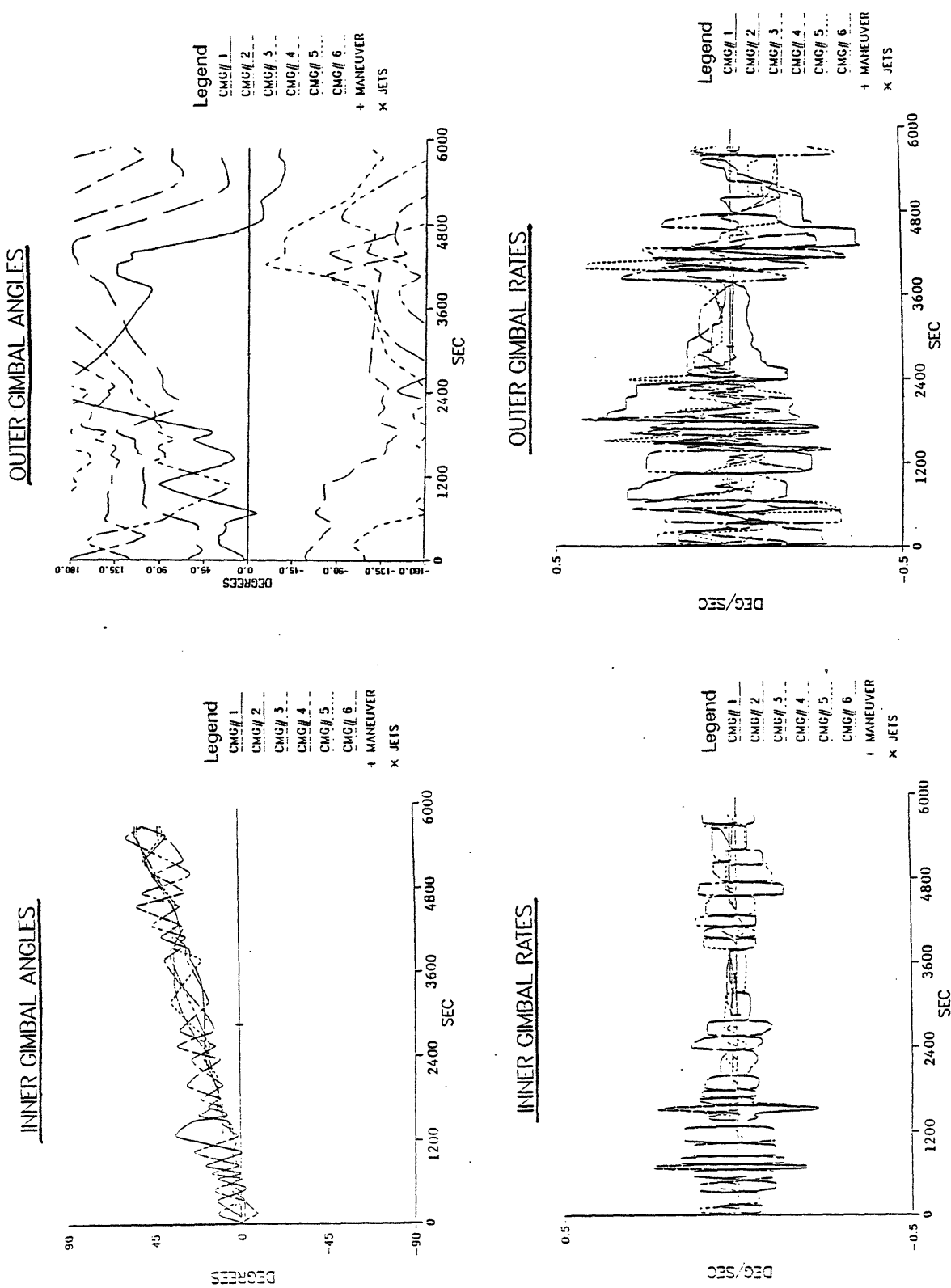


Fig. 12) LVLH Attitude Hold with Pitch Offset; Delta Torque Steering
Additional factor 50 gain on extreme negative costs

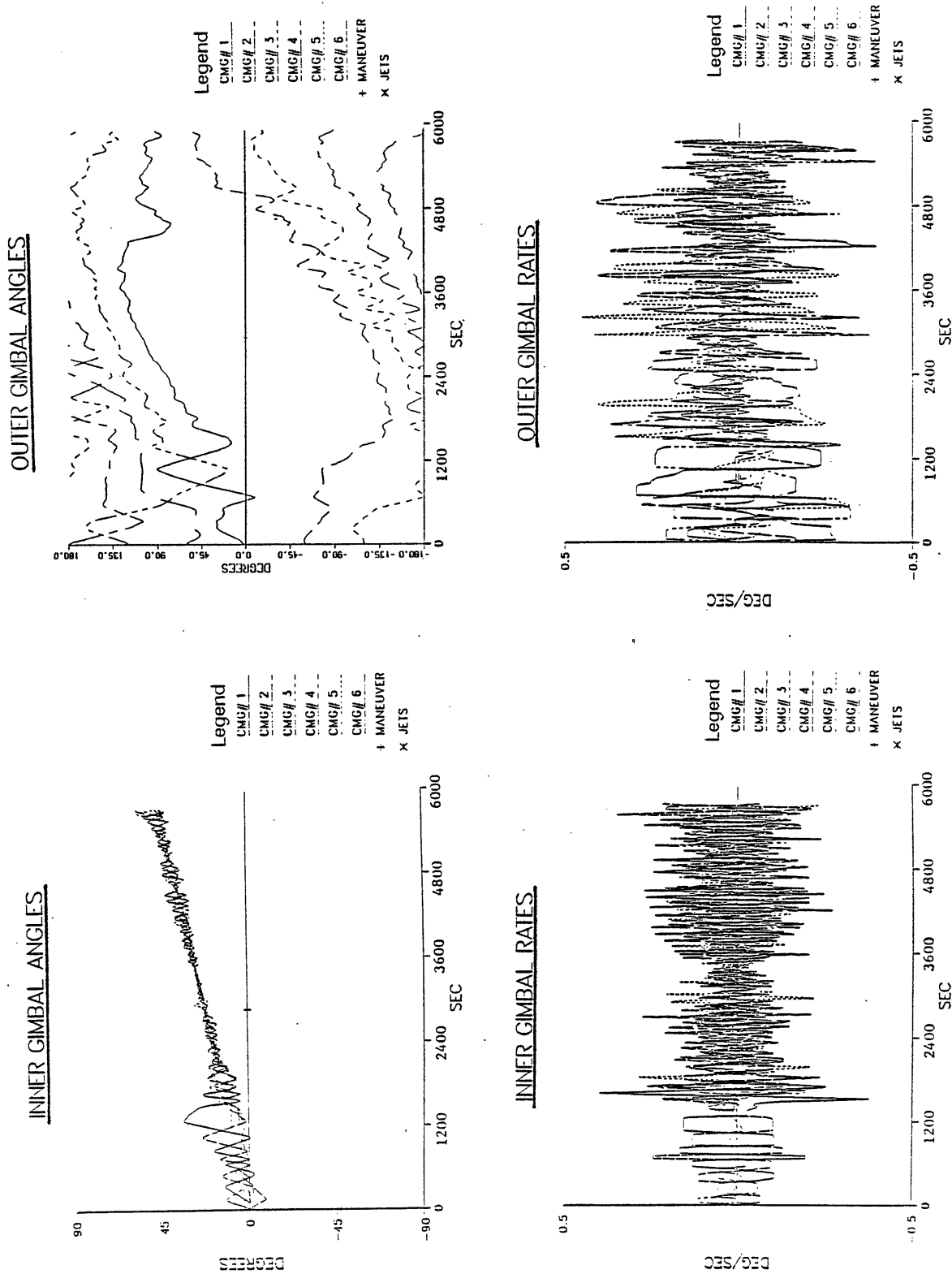
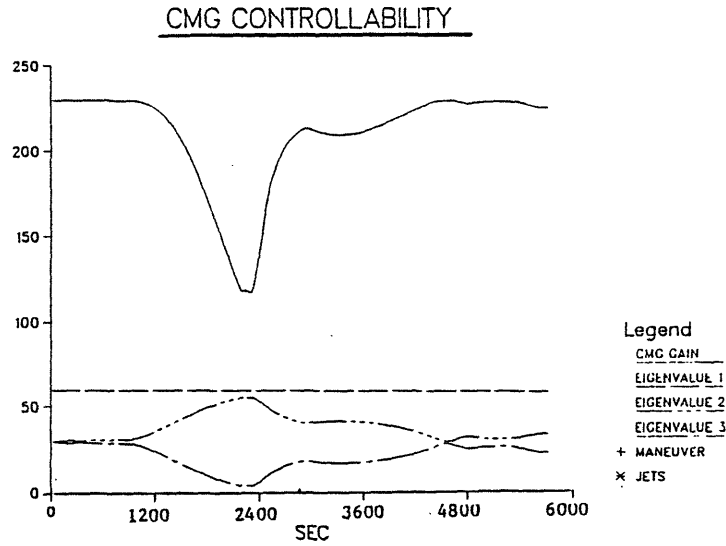
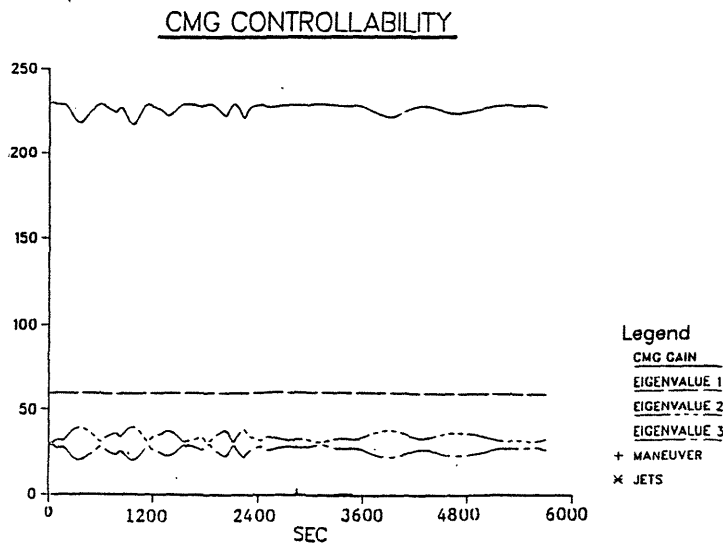


Fig. 13) 3-Axis CMG Controllability at TEA



ORBIT; TEA; STEER ABSOLUTE TORQUE



ORBIT; TEA; STEER DELTA TORQUE

CMG controllability parameters are plotted for the orbital runs of Fig. 5 (Absolute Torque Steering at Torque Equilibrium) and Fig. 7 (Damped Delta Torque Steering at Torque Equilibrium) in Fig. 13. The parameter of interest in these plots is the CMG gain (Eq. 44 of [2]), which represents the degree of 3-axis CMG controllability (this is the upper curve; high gain implies high controllability). The absolute torque method (top plot) shows a significant drop in CMG gain at $t \approx 2200$ sec. Observing the outer gimbals in Fig. 5, one can notice that this is due to the approach of a singular state with CMG #6 pointing antiparallel to all others. A delay in moving the outer gimbals of CMG #6 allowed this situation to occur (as it stands, it managed to move CMG #6 before the system actually went singular). This effect was also noted in [3] (Fig. 22), however the cost factors were adjusted differently in this case, and the rotor alignment did not become quite so critical.

The lower plot of Fig. 13 presents the controllability parameters produced under delta torque steering, using the same antilineup objective contribution. Here we see an essentially flat gain profile remaining at its maximum value; indeed, the omnipresent null motion performed under delta torque steering was able to dislodge the outer gimbal of CMG #6 before it approached the antiparallel orientation, creating a superior gimbal trajectory.

The above example supports the potential superiority of delta torque steering in singularity avoidance. Before definite conclusions are adopted in this area, however, additional studies should be performed.

4) Conclusions

The practical application of linear programming to CMG steering may require a means of smoothing the calculated gimbal rates. The simplest means of accomplishing this is to low-pass filter the gimbal rate output. If bandwidth and/or computational considerations preclude this option, changing decision variables to delta torque may also provide a more continuous gimbal rate profile. This strategy, however, requires additional logic to impose objectives onto gimbal motion and damp excessive gimbal activity. Methods to accomplish this were developed and tested in simulations; results indicated that delta torque steering could be applied successfully to yield lower gimbal chatter. If this method is adopted, however, deeper investigation should be performed into better damping of gimbal scissoring. Additional tweaking of upper bound attenuation and further adaptation of the objective function and linear program formulation could yield improvement over the results presented here (the effort described in this report constituted a quick study; a more

systematic look should be taken if the need for delta torque steering arises). Test results also seemed to indicate that the perpetual null motion performed under the delta torque formulation can move potentially hung gimbals into better orientations, enabling superior rotor lineup and singularity avoidance characteristics. Methods of slowing gimbal motion in the vicinity of momentum saturation were discussed; these ideas may be developed further if this proves to be problematic.

LIST OF REFERENCES

1. Paradiso, Joseph A., "A Highly Adaptable Steering/Selection Procedure for Combined CMG/RCS Spacecraft Control", *1986 AAS Guidance and Control Conf.*, Keystone CO., AAS 86-036, CSDL-P-2653, February, 1986.
2. Paradiso, Joseph A., "A Highly Adaptable Steering/Selection Procedure for Combined CMG/RCS Spacecraft Control", *Detailed Report*, CSDL-R-1835, March, 1986.
3. Paradiso, Joseph A., "Performance & Applications of a Hybrid Jet Selection & CMG Steering Law Based on Linear Programming", CSDL-R-1901, October, 1986.
4. Paradiso, Joseph A., "Selection and Management of Magnetically Gimballed CARES Gyroscopes via Linear Programming", 10C Space Station Memo 86-19, December, 1986.
5. Chung, A., *Linear Programming*, Charles E. Merrill Books, Inc., Columbus, Ohio, 1966.